PROCEEDINGS, TOUGH Symposium 2012
Lawrence Berkeley National Laboratory, Berkeley, California, September 17-19, 2012

NEAR-WELL PRESSURE DISTRIBUTION OF CO_2 INJECTION IN A PARTIALLY PENETRATING WELL

Edward Mehnert and Roland T. Okwen

University of Illinois at Urbana-Champaign, Prairie Research Institute, Illinois State Geological Survey
615 East Peabody Drive, Champaign, IL, 61820 USA
emehnert@illinois.edu and rokwen@illinois.edu

ABSTRACT

To mitigate global climate change, the atmospheric concentrations of greenhouse gases such as carbon dioxide, carbon monoxide, methane, and nitrous oxide must be reduced. Carbon dioxide (CO_2) can be captured and injected into subsurface reservoirs in a process known as geologic carbon sequestration (GCS). Geologic carbon sequestration in saline reservoirs offers the greatest storage capacity in the United States and worldwide. Numerical modeling offers planners a useful tool to evaluate the feasibility of GCS in saline and other reservoirs. With its database of CO_2 properties, TOUGH2 and its ECO2N module is an excellent simulator for evaluating the CO_2 movement in the subsurface.

Radial simulations (along the r-z axis) of brine injected into a thick saline reservoir show a smooth exponential increase in pressure over time near the injection well. However, CO_2 injected into a thick saline reservoir does not show the same smooth pressure increase. After some time, the pressure near the injection well levels off, remains steady, and then decreases slightly. The maximum pressure increase at the well is lower for CO_2 injection than for brine injection because brine is more viscous. In addition, the maximum pressure increase occurs before the end of the CO_2 injection period. Okwen et al. (2011) demonstrated this effect for fully penetrating wells and attributed this pressure response to the contrast in fluid density (native brine versus CO_2) and permeability anisotropy (horizontal to vertical permeability). In this paper, we seek to demonstrate that the effect is also observed in partially penetrating wells. Partially penetrating wells are important because they offer a well design that can maximize the storage volume of the buoyant CO_2 in thick reservoirs.

We used TOUGH2 and the ECO2N module to conduct numerical experiments to evaluate the pressure response of injecting CO_2 and brine into saline reservoirs. Preliminary results confirm the results of Okwen et al. (2011) for partially penetrating wells. For a well perforated in the bottom of an anisotropic injection formation, CO_2 injection leads to lower pressures near the injection well perforations but higher injection pressures near the top of the injection formation. Apparently, vertical transport is more significant with CO_2 injection than brine injection, and it alters the pressure profile near the injection well. These results could inform how partially penetrating wells are completed.

INTRODUCTION

Geologic carbon sequestration (GCS) in saline reservoirs offers the greatest storage capacity for greenhouse gases in the United States and worldwide (IPCC, 2005). Numerical modeling offers planners a useful tool to evaluate the feasibility of GCS in saline and other reservoirs. However, numerical simulation of two-phase flow for large geographic areas such as geologic basins can be computationally demanding (thus expensive) and technically demanding. In an attempt to simplify the task of basin-scale modeling, researchers (e.g., Nicot 2008) have suggested that basin-scale simulations could be simplified by injecting brine instead of CO_2. This approach is considered to be adequate if one is interested in studying the far field effects of GCS. Motivated by this concept, we conducted numerical simulations to help define “far field” and “near field” in this context.

Okwen et al. (2011) conducted numerical experiments to study temporal variations in the near-wellbore pressures for a fully penetrating well. They found that temporal variations in pressure near the wellbore depend strongly on the density contrast between the injected and native fluids and vertical anisotropy of the injection formation. Because partially penetrating wells offer a technology to fully utilize the reservoir pore space at GCS sites, we have conducted numerical experiments to explore these temporal variations for partially penetrating wells.

APPROACH

To compare the effects of injecting CO_2 and brine into a deep saline reservoir, a number of simulations were conducted. The simulations were set up using two-dimensional radial grids. The reservoir was assumed to be 50 to 100 m thick and to extend 100,000 m, and have an infinite volume element at this distant boundary. In each case, 1 million tonnes of fluid were injected per year for 10 years. Each modeling scenario evaluated 10 years of fluid injection followed by 40 years of post-injection. The horizontal permeability was set at 4.94×10^{-12} m^2 while the vertical permeability varied (4.94×10^{-14} m^2 to 4.94×10^{-13} m^2). The reservoir thickness and perforated thickness were varied as shown in Table 1. Fluid was injected at the bottom of a deep saline reservoir for the reservoir conditions defined in Table 2. To evaluate the effect that fluid properties have on the pressure response in the injection zone, we conducted a number of simulations using CO_2, high-density CO_2, water, and brine. The density and dynamic viscosity of these fluids at formation pressure and temperature are given in Table 3. As introduced by Okwen et al. (2011), high-density CO_2 is a hypothetical fluid with density equal to that of water and viscosity equal to that of CO_2 which allows us to evaluate the effect of viscosity.

Table 1. Scenarios investigated

Reservoir thickness (m)	Perforated thickness (m)		
	10	25	50
50	RS9a	RS9b	
100	RS9c		RS9d

With its database of CO_2 properties, TOUGH2 (Pruess et al., 1999) and its ECO2N module (Pruess, 2005) is an excellent simulator for evaluating the CO_2 movement in the subsurface. A numerical grid with 50 layers and 53 columns was used, which has 2,650 elements. The grid spacing in the radial direction increased logarithmically from the injection well to the distant boundary. The reservoir was assumed to have a single rock type and was bounded by no-flow boundaries at the top and bottom.

Table 2. Reservoir conditions and TOUGH2 input

Parameter	Value
Dimensions (r x Z, m)	100,000 x 50 or 100
Gridblocks (r x Z)	53 × 50
Horizontal permeability (m^2)	4.94×10^{-12}
Vertical permeability (m^2)	4.94×10^{-13} to 4.94×10^{-14}
Porosity (%)	16
Pore compressibility (Pa^{-1})	3.71×10^{-10}
Temperature (°C)	49.2
Salt mass fraction	0.20
Dissolved CO_2	0
Relative permeability function	
Residual liquid saturation	0.30
Residual gas saturation	0.25
Exponent (λ)	0.40
Capillary pressure function	
Exponent (λ)	0.40
Residual liquid saturation	0.00
Strength coefficient (Pa^{-1})	5.0×10^{-5}
Maximum capillary pressure (Pa)	5.0×10^{5}

Table 3. Properties of injected fluids at formation pressure and temperature (19.6 MPa and 49.2°C)

Fluid	Density (kg/m^3)	Viscosity (Pa sec)
Brine	1140.4	7.8×10^{-4}
CO_2	786.8	6.9×10^{-5}
High-density CO_2	996.5	6.9×10^{-5}
Water	996.0	5.6×10^{-4}

Note: CO_2 viscosity data from Fenghour et al. (1998)

Relative permeability was defined using the van Genuchten (1980)-Mualem (1976) function for liquids and Corey (1954) for gas. Capillary pressure was defined using the van Genuchten (1980) function with the parameters defined in Table 2.

RESULTS

First, the TOUGH2 simulation results regarding the pressure response in the injection zone will be discussed, demonstrating the effect of the injected fluid, formation thickness and perforation ratio. Next, more detail will be provided for a single scenario where four types of fluid were injected to demonstrate the significance of fluid density and viscosity on the predicted pressure changes.

Effect of Perforation Ratio

In Scenario 9a, the injection zone is 20% perforated, with the lowermost 10 m of the 50 m injection zone accepting the injected fluid (Table 1). In Figure 1a, the pressure at the top of the injection zone (index= 1) is shown for two simulations—when brine is injected and when CO_2 is injected. In addition, the gas saturation curve shows the movement of CO_2 to the top of the injection zone over time. The gas rises quickly through this thin reservoir but does not reach maximum saturation until after the injection period ends (t = 3652.5 days). Pressure at the top of the injection zone is predicted to be higher during the injection period when CO_2 is injected than when brine is injected. Also, at this location, the time to reach maximum pressure is significantly different for the two fluids. During the post-injection period, CO_2 injection leads to higher pressures than those predicted for brine injection. An inverse pattern is observed at the bottom of the injection zone (index = 50) (Figure 1b). Here, we see that brine injection leads to higher pressures during the injection period. During the post-injection period, the formation pressure is higher for CO_2 injection than brine injection, but the difference is much smaller.

When the perforated thickness is increased to 50% in Scenario 9b (25 m of 50 m reservoir is perforated), the predicted pressures at the top of the injection zone are similar to Scenario 9a, but the pressures are lower at the bottom of the reservoir (Figures 2a and 2b). The maximum gas saturation at the top of the injection zone in Scenario 9b exceeds that predicted in 9a.

Another way to evaluate the TOUGH2 output is to examine the normalized pressure difference which is defined as:

$$\Delta P_{norm} = {(P_{CO_2} - P_{brine})}\Big/{P_{brine}(t=0)} \qquad (1)$$

The normalized pressure differences for four scenarios are shown in Figure 3. The graphs show the pressure difference at the top (index 1), middle (index 25) and bottom (index 50) of the injection zone. The fourth location is generally near the middle of the perforated zone (index 45). The pressure difference tends to be positive for the two higher locations and negative for both lower locations. The magnitude of the negative values generally exceeds the magnitude of the positive values.

Effect of Fluid Density and Viscosity

Using Scenario 9a, four different fluids were injected. The normalized pressure differences versus time are shown in Figure 4. Figure 4a shows the pressure difference for the CO_2 and brine simulations. Figure 4b shows the pressure difference for the high-density CO_2 and brine simulations. Figure 4c shows the pressure difference for the water and brine simulations. The pressure differences have the greatest magnitude for CO_2 and brine, while the pressure difference has the smallest magnitude for the water and brine. The differences are greatest early in the injection period for the higher locations, and toward the end of the injection period for the lower locations.

DISCUSSION

The TOUGH2 results shown in Figure 1 demonstrate that injecting CO_2 (rather than injecting brine) via a partially penetrating well leads to higher pressures in the upper portion of the injection zone, but lower pressures in the lower portion of the injection zone due to buoyancy of CO_2. The highest pressures in the upper portion of the injection zone occur early in the injection period, while highest pressures in the lower portion of the injection zone occur at the end of the injection period. The magnitude of the pressure differences, especially those predicted for the lower portion of the injection zone, appears to be a function of the injection zone thickness (compare 9b and 9d), perforation ratio (compare 9a vs 9b and 9c vs 9d), and the anisotropy ratio (data not shown).

The difference in pressures predicted by TOUGH2 (Figure 4) are due to differences in fluid viscosity and density. Water has a lower density and similar viscosity to the brine, while

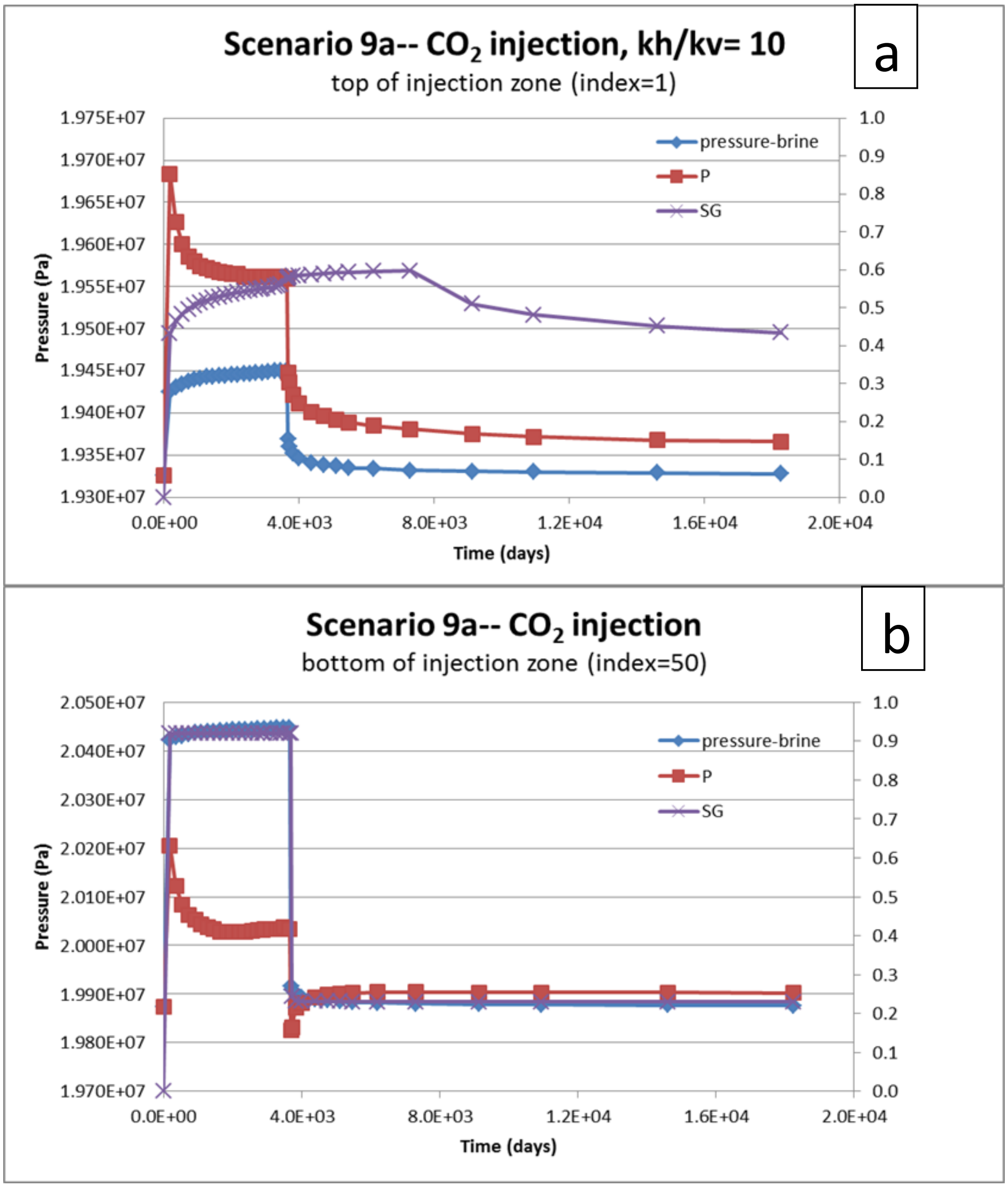

Figure 1. Results for modeling Scenario 9a (perforation thickness = 10 m, reservoir thickness = 50 m). Results are shown for the top of the injection zone (1a) and the base of the injection zone (1b). Fluid is injected from 0 to 3,652.5 days. Figure abbreviations: P = pressure resulting from CO_2 injection & SG = gas or CO_2 saturation which can vary from 0 to 1.0.

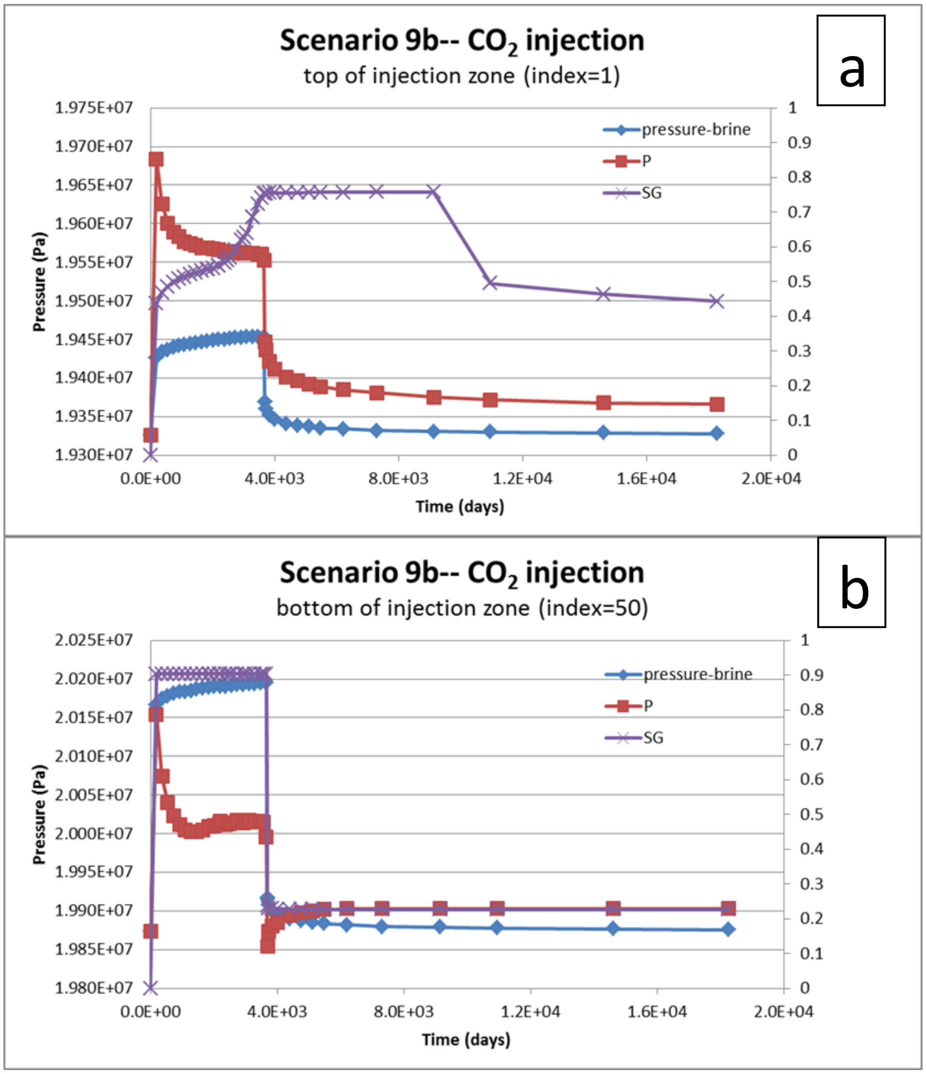

Figure 2. Results for modeling Scenario 9b (perforation thickness = 25 m, reservoir thickness = 50 m). Results are shown for the top of the injection zone (2a) and the base of the injection zone (2b). Fluid is injected from 0 to 3,652.5 days.

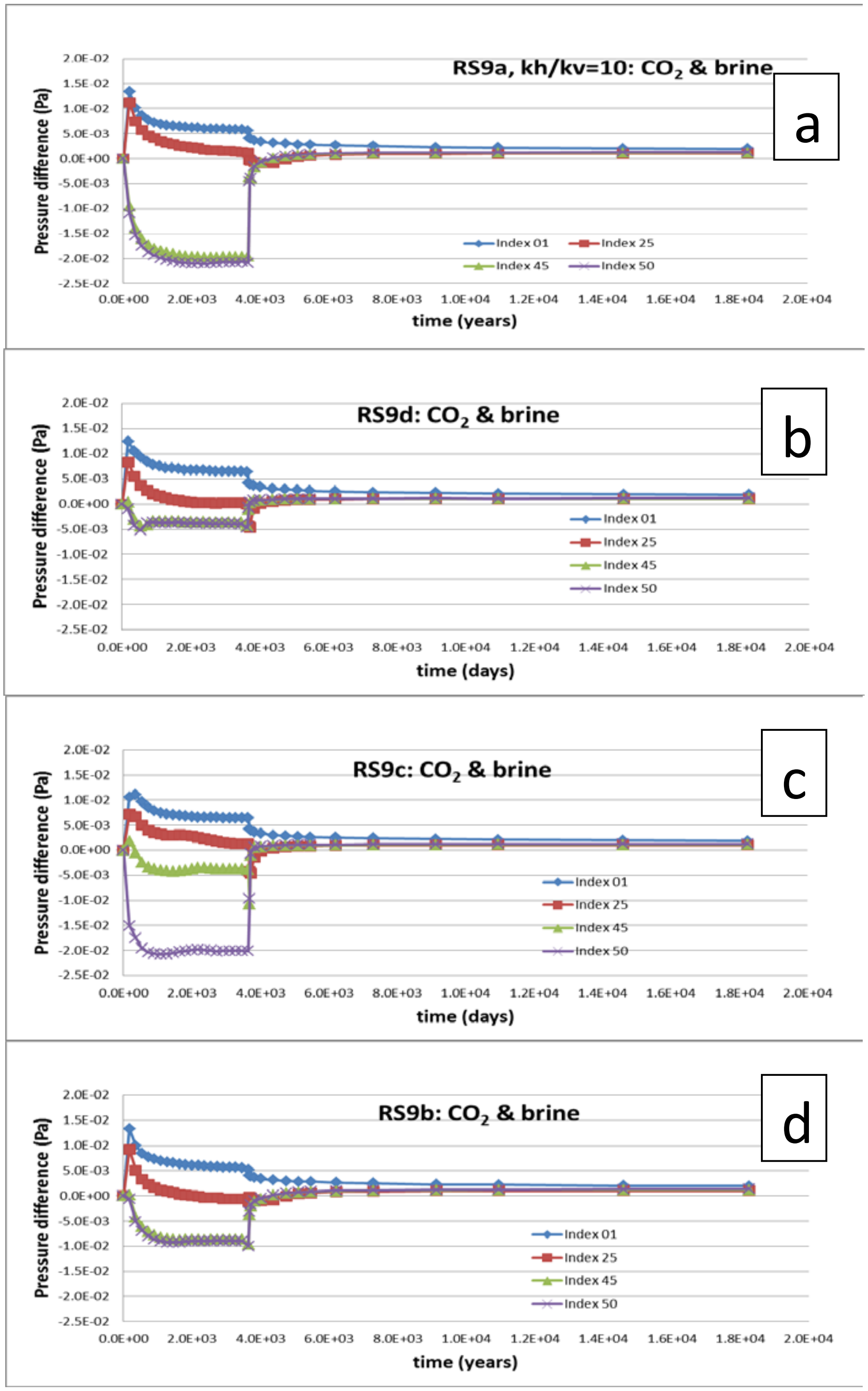

Figure 3. Normalized pressure difference for four scenarios, which shows the difference in the pressure when CO_2 and brine are injected. Data are provided at the top (index 1), middle (index 25) and bottom (index 50) of the injection zone and near the middle of the perforated zone (index 45).

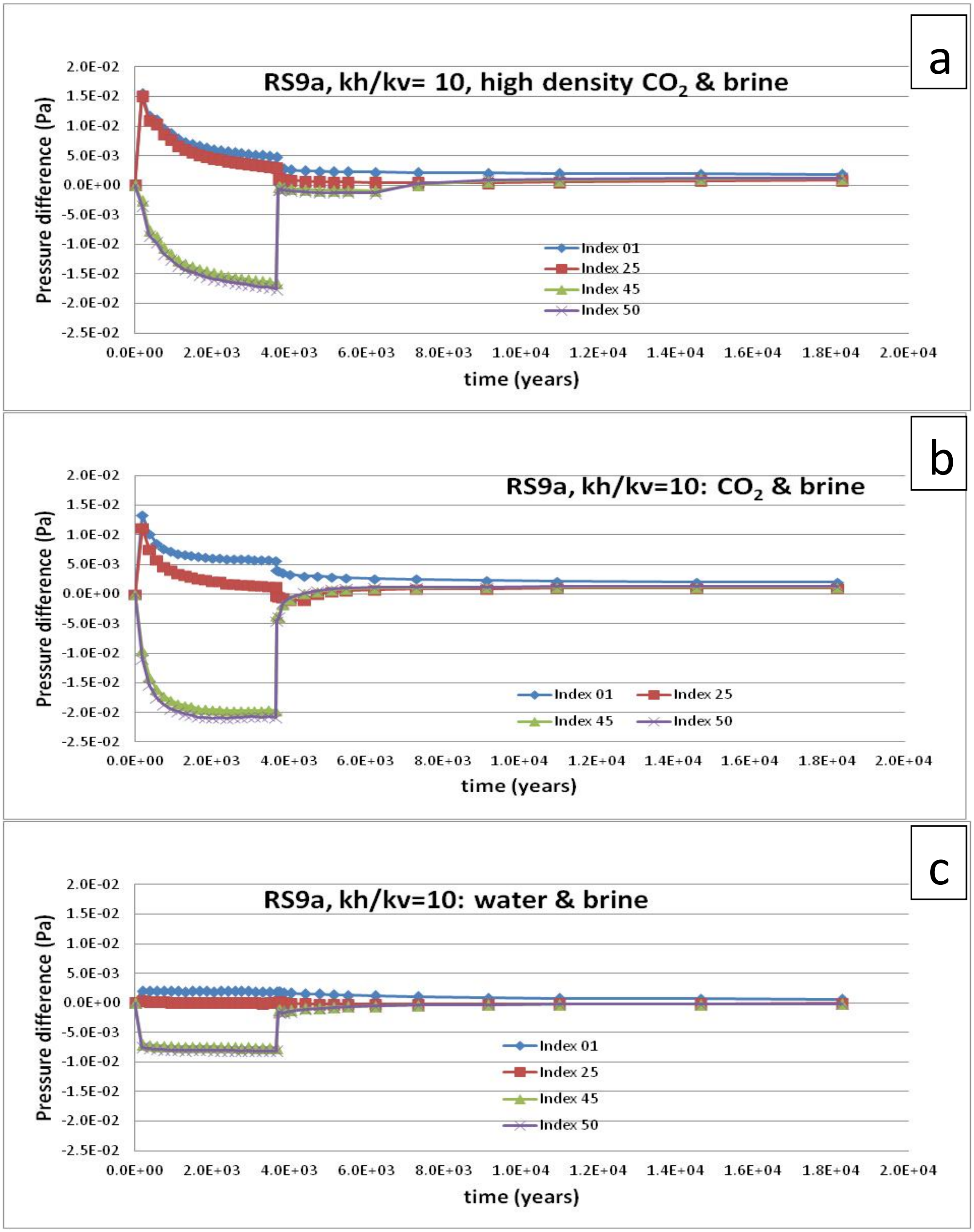

Figure 4. Normalized pressure difference for three fluids (CO_2, high-density CO_2 and water) compared to brine injection.

CO_2 has a lower density and viscosity. Figure 4c demonstrates the effect of fluid density on pressure. Injecting a denser fluid (brine) causes higher pressure in the lower portion of the injection zone, but very little effect on pressure in the upper portion of the injection zone. In addition, the density difference leads to a steady change in pressure in the lower portion of the injection zone. Comparing Figures 4b and 4c demonstrates the effect of fluid viscosity. The magnitude of the pressure difference changes in the upper and lower portion of the injection zone and its effects change over time. The combined effect of fluid density and viscosity can be observed in Figure 4a.

For the scenarios modeled, differences in near-well pressure profiles were observed when brine and CO_2 were injected via partially penetrating wells. The pressure profile near the well depends on fluid viscosity, fluid density, injection zone thickness, and other parameters such as formation permeability. The maximum pressure difference predicted in the upper portion of the injection zone seems small (<2% of the initial formation pressure), but it might be significant in terms of cap-rock integrity. The pressure increase is likely a function of formation permeability and should be investigated further for scenarios with more realistic permeability values (4.9×10^{-15} to 4.9×10^{-13} m^2 or 5 to 500 md).

ACKNOWLEDGMENTS

Publication authorized by the Director, Illinois State Geological Survey.

REFERENCES

Corey, A.T., The interrelation between gas and oil relative permeabilities, *Producers Monthly 19*(1): 38-41, 1954.

Fenghour, A., W.A. Wakeham and V. Vesovic, The viscosity of carbon dioxide. *Journal of Physical and Chemical Reference Data 27*(1): 31-44, 1998.

Intergovernmental Panel on Climate Change (IPCC), *IPCC Special Report on Carbon Dioxide Capture and Storage*. New York: Cambridge University Press, 2005.

Mualem, Y., New model for predicting hydraulic conductivity of unsaturated porous media, *Water Resources Research 12*(3): 513-522, 1976

Nicot, J.-P., Evaluation of large-scale CO_2 storage on fresh-water sections of aquifers: An example from the Texas Gulf Coast Basin. *International Journal of Greenhouse Gas Control 2*(4): 582-593, 2008.

Okwen, R.T., M.T. Stewart and J.A. Cunningham, Temporal variations in near-wellbore pressures during CO_2 injection in saline aquifers, *International Journal of Greenhouse Gas Control 5*(5): 1140-1148, 2011.

Pruess, K., C. Oldenburg, and G. Moridis, *TOUGH2 User's Guide, Version 2.0*, Report LBNL-43134, Lawrence Berkeley National Laboratory, Berkeley, Calif., 1999.

Pruess, K., *ECO2N: A TOUGH2 fluid property module for mixtures of water, NaCl, and CO_2*, Earth Sciences Division, Lawrence Berkeley National Laboratory, Report LBNL-57952, 2005.

van Genuchten, M.T., A closed-form equation for predicting the hydraulic conductivity of unsaturated soils. *Soil Science Society of America Journal 44*(5): 892-898, 1980.